Singularity Surfaces and Maximal Singularity-Free Boxes in the Joint Space of Planar 3-RPR Parallel Manipulators

Mazen Zein, Philippe Wenger, Damien Chablat

12th IFToMM World Congress, Besançon (France), June18-21, 2007

Singularity Surfaces and Maximal Singularity-Free Boxes in the Joint Space of Planar 3-*RPR* Parallel Manipulators

Mazen ZEIN Philippe WENGER Damien CHABLAT
IRCCyN, Institut de recherche en communications et cybernéthique de Nantes
1, rue de la Noe, 44322 Nantes

Abstract— *In this paper, a method to compute joint space singularity surfaces of 3-RPR planar parallel manipulators is first presented. Then, a procedure to determine maximal joint space singularity-free boxes is introduced. Numerical examples are given in order to illustrate graphically the results. This study is of high interest for planning trajectories in the joint space of 3-RPR parallel manipulators and for manipulators design as it may constitute a tool for choosing appropriate joint limits and thus for sizing the link lengths of the manipulator.*

Keywords: *3-RPR* parallel manipulators, singularity, singularity-free zones, joint space, joint limits.

I. Introduction

Most parallel manipulators have singularities that limit the motion of the moving platform. The most dangerous ones are the singularities associated with the direct kinematics, where two assembly-modes coalesce. Indeed, approaching such a singularity results in large actuator torques or forces, and in a loss of stiffness. Hence, these singularities are undesirable. There exists three main ways of coping with singularities, which have their own merits. A first approach consists in eliminating the singularities at the design stage by properly determining the kinematic architecture, the geometric parameters and the joint limits [4,4,7]. This approach is safe but difficult to apply in general and restricts the design possibilities. A second approach is the determination of the singularity-free regions in the workspace [5,15-17,20,24]. This solution does not involve a priori design restrictions but, because of the complexity of the singularity surfaces, it may be difficult to determine definitely safe regions. Finally, a third way consists in planning singularity-free trajectories in the manipulator workspace [2,6,19]. With this solution one is also faced with the complexity of the singularity equations but larger zones of the workspace may be exploited.

In this paper, we choose to use the second approach by determining maximal joint space singularity-free boxes. This approach will help us determine appropriate joint limits and link dimensions.

Planar parallel manipulators and particularly manipulators with three extensible leg rods, referred to as 3-*RPR*, have received a lot of attention because they have interesting potential applications in planar motion systems [9,21]. As shown in [18], moreover, the study of the 3-*RPR* planar manipulator may help better understand the kinematic behavior of its more complex spatial counterpart, the 6-dof octahedral manipulator, which has also triangular base and platforms.

The singularities of these manipulators have been most often represented in their workspace [13,14,18] but more rarely in their joint space [18,24,26].

Hunt and Primrose showed that 3-*RPR* planar manipulator could have up to 6 assembly-modes [12]. Mcaree and Daniel analyzed the joint space singularities through slices to explain non-singular changing trajectories [188], and Zein et al analyzed the topology of these slices in [26]. It was shown in [18,24,25] that, to change its assembly mode without meeting a singularity, a *3-RPR* manipulator should encircle a cusp point in its joint space.

In this paper, a method to compute and to represent joint space singularities of 3-*RPR* planar parallel manipulators is first proposed. A procedure is then provided to determine maximal joint space singularity-free boxes.

This work is of a high interest for the determination of appropriate joint limits and for planning trajectories in the joint space.

II. Manipulators under study

The manipulators under study are 3-DOF planar parallel manipulators with three extensible leg rods (Fig.1). These manipulators have been frequently studied and have interesting potential applications in planar motion systems. The geometric parameters are the three sides of the moving platform d_1, d_2, d_3 and the position of the base revolute joint centers defined by A_1, A_2 and A_3. The reference frame is centered at A_1 and the x-axis passes through A_2. Thus, $A_1 = (0, 0)$, $A_2 = (A_{2x}, 0)$ and $A_3 = (A_{3x}, A_{3y})$. The parameter β is function of d_1, d_2 and d_3.

The joint space $\boldsymbol{Q}$ is defined by the vectors of the lengths of the three actuated extensible links $\dot{\mathbf{q}} = \begin{bmatrix} \dot{\rho}_1 & \dot{\rho}_2 & \dot{\rho}_3 \end{bmatrix}^{\mathrm{T}}$.

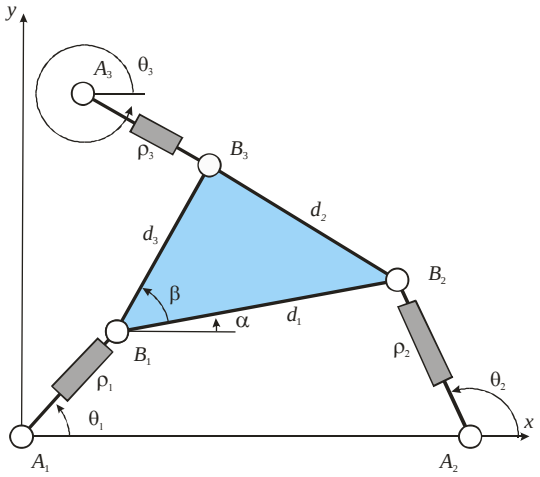

Fig. 1. A 3-*RPR* parallel manipulator

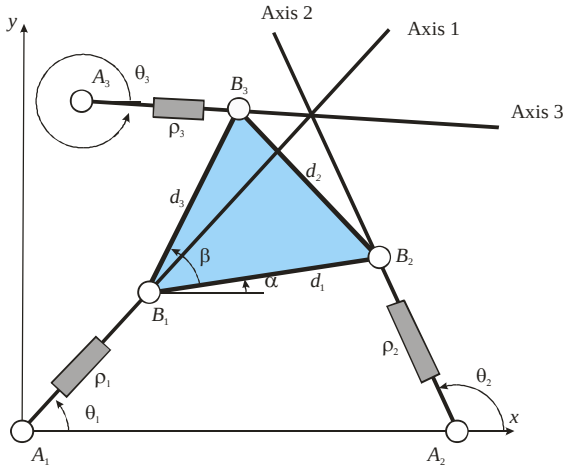

Fig. 2. A 3-*RPR* parallel manipulator on a singular configuration.

III. Kinematics of 3-*RPR* parallel manipulators

The relation between the joint space **Q** and the workspace **W** can be expressed as a system of non-linear algebraic equations, which can be written as:

$$F(\mathbf{x}, \mathbf{q}) = 0 \tag{1}$$

where **x** and **q** are respectively the vectors of the workspace and joint space variables.

Differentiating equation (1) with respect to time leads to the velocity model:

$$\mathbf{A}\mathbf{t} + \mathbf{B}\dot{\mathbf{q}} = \mathbf{0} \tag{2}$$

where $\mathbf{t} = \left[w \ \dot{\mathbf{c}}\right]^T$ (w is the scalar angular velocity and $\dot{\mathbf{c}}$ is the two-dimensional velocity vector of the operational point B_1 of the platform if we used the first workspace parameters), **A** and **B** are 3×3 Jacobian matrices which are configuration dependent, and $\dot{\mathbf{q}} = \left[\dot{\rho}_1 \quad \dot{\rho}_2 \quad \dot{\rho}_3\right]^T$ is the joint velocity vector.

IV. Joint space singularities of 3-RPR parallel manipulators

The singularities of 3-DOF planar parallel manipulators have been extensively studied (see for example [3,8,14,18,22]). They were defined in the workspace (x, y, α) and to the author's knowledge, there exist a small number of works dealing with the singular configurations in the manipulators joint space (ρ_1, ρ_2, ρ_3).

In a parallel singularity, matrix **A** is singular. To derive the singularity equations, it is usual to expand the determinant of **A**. We use rather a geometric approach that does not involve complicated algebraic calculus. The *3-RPR* parallel manipulator is in a singular configuration whenever the axes of its three legs are concurrent or parallel [11] (Fig. 2).

In order to derive this geometric condition, we derive the condition for the three leg axes to intersect at a common point (possibly at infinity). We first write the equations of the three leg axes:

$$\begin{cases} (\text{Axis 1}) : y\cos(\theta_1) = x\sin(\theta_1) \\ (\text{Axis 2}) : y\cos(\theta_2) = (x - A_{2x})\sin(\theta_2) \\ (\text{Axis 3}) : y\cos(\theta_3) = (x - A_{3x})\sin(\theta_3) + A_{3y}\cos(\theta_3) \end{cases} \tag{3}$$

Eliminating x and y yields the following singularity equation in the task parameters (θ_1, θ_2, θ_3):

$$A_{2x}s_2s_{31} + \left(A_{3x}s_3 - A_{3y}c_3\right)s_{12} = 0 \tag{4}$$

where $s_i = \sin\left(\theta_i\right)$, $c_i = \cos\left(\theta_i\right)$ and $s_{ij} = \sin\left(\theta_i - \theta_j\right)$.

It is possible to express Eq. (4) as a function of the joint space parameters ρ_1, ρ_2 and ρ_3 by using the constraint equations of the *3-RPR* manipulator. However, the resulting equation would be too complicated to yield real insights, and difficult to handle.

Our approach to compute the singular configurations in the joint space consists in reducing the dimension of the problem by first considering two-dimensional slices of the configuration space by fixing the first leg rod length ρ_1. The singular surfaces in the full joint space are then calculated by "stacking" the slices.

Step 1: We rewrite Eq. (4) as a function of ρ_1, α and θ_1 using the constraint equations of the manipulator.

$$\begin{cases} A_{2x} + \rho_2 c_2 - \rho_1 c_1 - d_1\cos\left(\alpha\right) = 0 \\ \rho_2 s_2 - \rho_1 s_1 - d_1\sin\left(\alpha\right) = 0 \\ A_{3x} + \rho_3 c_3 - \rho_1 c_1 - d_3\cos\left(\alpha + \beta\right) = 0 \\ A_{3y} + \rho_3 s_3 - \rho_1 s_1 - d_3\sin\left(\alpha + \beta\right) = 0 \end{cases} \tag{5}$$

The first (respectively last) two equations make it possible to express ρ_2 (respectively ρ_3) as function of ρ_1, α and θ_1. Then, c_2 and s_2 (respectively c_3 and s_3) are calculated as function of ρ_1, α and θ_1 from the first (respectively last)

two equations of (5) and their expressions are input in Eq. (4), which, now, depend only on L_1, α and θ_1.

Step 2: We fix a value for ρ_1, so Eq. (4) depends now only on α and θ_1. By varying α or θ_1, we compute the roots of the equation, to obtain the singular configurations (α_s, θ_{1s}) for a fixed ρ_{1s}.

Step 3: For every singular configuration computed in the space (α, θ_1) in the second step of the approach, we calculate the corresponding values ρ_{2s} and ρ_{3s} using the equation system (6). We have thus the singular configurations curves in a slice of the joint space (ρ_2, ρ_3) with ρ_1 fixed.

$$\begin{cases} \rho_2 = \sqrt{\left(-A_{2x} + \rho_1\cos(\theta_1) + d_1\cos(\alpha)\right)^2 + \left(\rho_1\sin(\theta_1) + d_1\sin(\alpha)\right)^2} \\ \rho_3 = \sqrt{\left(A_{3x} - \rho_1\cos(\theta_1) - d_3\cos(\alpha+\beta)\right)^2 + \left(A_{3y} - \rho_1\sin(\theta_1) - d_3\sin(\alpha+\beta)\right)^2} \end{cases} \quad (6)$$

Figure 3 shows a slice of the joint space singular configurations for ρ_1=17 obtained for the same 3-*RPR* manipulator used in [14,18,21]. We refer only to this manipulator in this paper in order to illustrate our work. The geometric parameters of this manipulator are recalled below in an arbitrary length unit:

A_1=(0, 0)	d_1=17.04
A_2=(15.91, 0)	d_2=16.54
A_3=(0, 10)	d_3=20.84

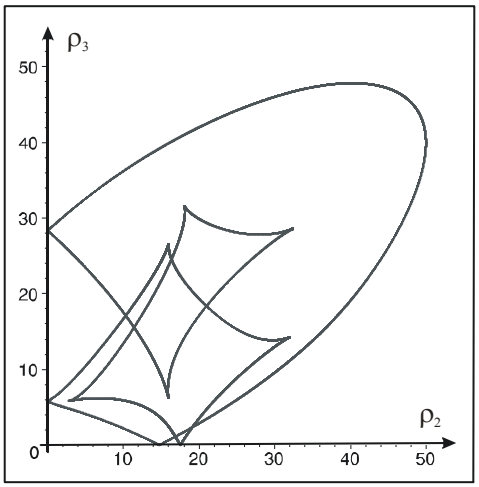

Fig. 3. Singular configurations in (ρ_2, ρ_3) for ρ_1=17.

Step 4: We compute the joint space singularity slices for a number of ρ_1 values, to do this we have to repeat steps 2 and 3 while varying ρ_1.

Finally, we collect all the computed slices in one file to obtain the singularities in the joint space (ρ_1,ρ_2, ρ_3).

Figure 4 represents the singularities in the joint space of the manipulator studied when ρ_1 varies from 0 to 50. To obtain this surface, we have imported the solutions obtained in step 4 into a CAD software, and we have meshed them together.

Obviously, there is continuity between the singularities slices, one can claim, without any doubt, that there is singularity between the different slices.

The surface depicted in Fig. 4 is of interest:

i. for planning trajectories in the joint space because it shows clearly the joint space regions that are free of singularities.

ii. for manipulator design, because it constitutes a tool for defining the values of the joint limits such that the joint space is a singularity-free box.

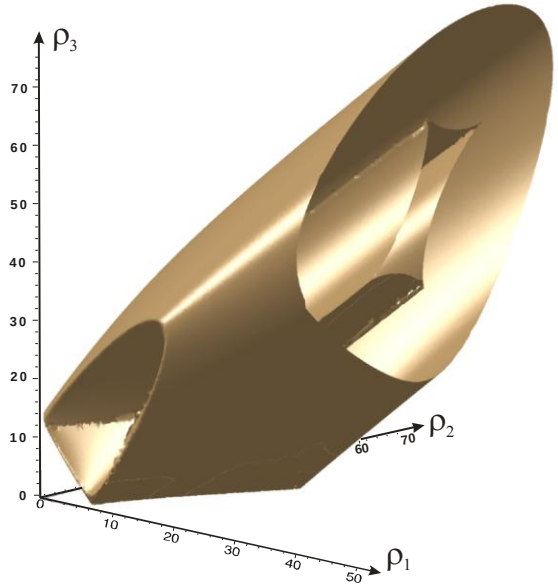

Fig. 4. Joint space singularity surfaces of the 3-*RPR* manipulator studied when ρ_1 varies from 0 to 50.

V. Maximal joint space singularity-free boxes

In a context of design and/or trajectory planning, an important problem is to find singularity-free zones in the joint space.

In this section, we introduce a new procedure to determine maximal singularity-free boxes in the joint space of *3-RPR* manipulators. These singularity-free boxes will help us fix the manipulator joints limits.

Two numerical examples are provided to illustrate the effectiveness of the procedure.

A. Procedure

Step 1: We choose an initial joint space configuration $Q_0(\rho_{10},\rho_{20},\rho_{30})$. This configuration can be chosen according to several considerations, for example choosing Q_0 as the image through the inverse kinematics of a prescribed workspace center, or choosing it directly in the joint space as the center of a large singularity-free zone.

Step 2: We calculate the largest singularity-free cube centered at $Q_0(\rho_{10},\rho_{20},\rho_{30})$.

To do this, we calculate the infinity norm distance *d*, also known as Chebyshev distance, between the center point $Q_0(\rho_{10},\rho_{20},\rho_{30})$ and each of the joint space singular points $Q_s(\rho_{1s},\rho_{2s},\rho_{3s})$ computed in Section IV:

$$d = \max\left(\left|\rho_{10}-\rho_{1s}\right|,\left|\rho_{20}-\rho_{2s}\right|,\left|\rho_{30}-\rho_{3s}\right|\right) \quad (7)$$

and we keep the minimal distance d_{min} found over all, because we are searching for the distance between the closest joint space singularity configuration Q_s from the center point Q_0.
The length of the singularity-free cube edge *a* will be:

$$a = 2\times d_{min} \quad (8)$$

Step 3: The choice of the initial center point $Q_0(\rho_{10},\rho_{20},\rho_{30})$ does not lead to an optimized solution, in other words varying lightly the center point position may lead to a largest singularity-free cube. Thus, the position of the initial point must be optimized, which we have done using a Hooke and Jeeves optimization scheme [10]. Note that the solution found is a local optimum.
Step 4: The cube found in step 3 touches the closest singular configuration to the center point. In order that the cube does not touch the singularities surface and for more security we subtract a small security value *s* from the distance d_{min}. Such a value can be related to laws of command to stop the motion when the joint velocity is maximum.

The manipulator joint limits corresponding to the cube found can be easily computed as follows:

$$\begin{cases}\rho_{i\min} = \rho_{i0} - \left(d_{\min} - s\right)\\ \rho_{i\max} = \rho_{i0} + \left(d_{\min} - s\right)\end{cases} \quad \text{with } i=1,2,3 \quad (9)$$

B. Application of the procedure

In this section, two examples are provided in order illustrate the application of the procedure.

Example 1:
For the same manipulator studied, we consider the center point $Q_0(35,25,45)$ in the joint space. This point was chosen in the center of a large singularity-free zone in the joint space. By computing the Chebyshev distances between each joint space singular point Q_s computed in section IV, and Q_0, the minimal distance obtained is d_{min}=5.3, so the edge length of the singularity-free cube is a = 10.6.
By running the optimization algorithm, we find a maximal value d_{min}=7.175 for a center point Q(*41.625, 24.875, 44.125*).
We subtract a security value of 0.1 from d_{min} which becomes d_{min}=7.075.
Figure 5 shows the joint space singularity surface and the maximal joint space singularity-free cube centered at Q(*41.625, 24.875, 44.125*) for the manipulator studied.

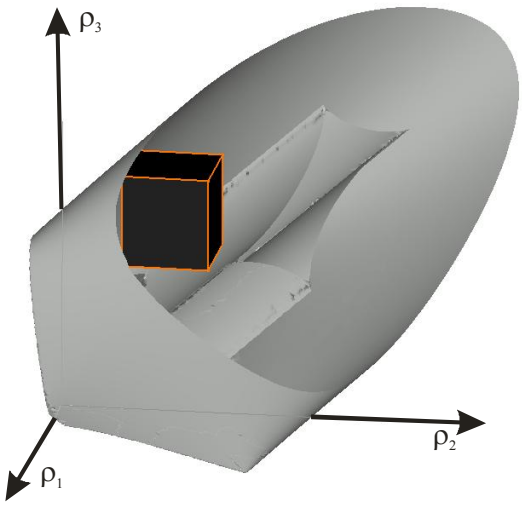

Fig. 5. Joint space singularity surfaces and maximal joint space singularity-free cube centered at Q(*41.625, 24.875, 44.125*).

Figures 6 shows the images through the direct kinematics of the maximal joint space singularity-free cube, which are two separate singularity-free components, each of them being located in an aspect of the workspace [24]. The projections of these two components onto the (x,y) plane are plotted in gray in Figure 6.

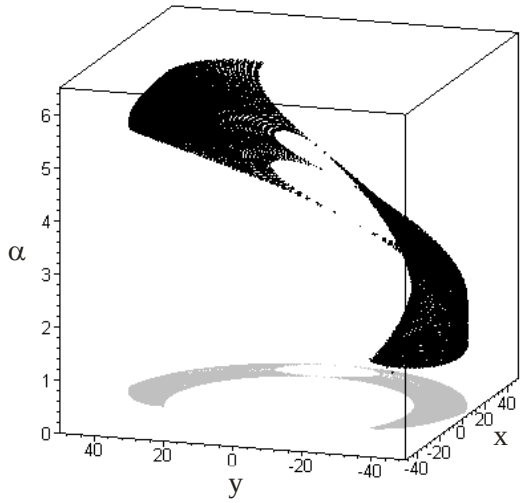

Fig. 6. Images by direct kinematics of the joint space singularity-free cube (in black), and their projection on the (x,y) plane (in gray).

Figures 7 shows the two workspace components and the workspace singularities of the *3-RPR* manipulator studied, the singularities are plotted in color.

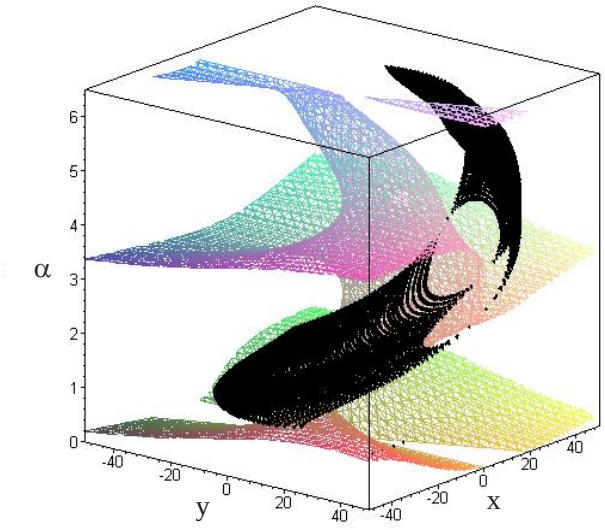

Fig. 7. Singularity-free components with workspace singularities.

Example 2:

For the same manipulator, we consider in this example the center point $Q_0(30,50,35)$ in the joint space. By computing the Chebyshev distances between each joint space singular point Q_s computed in Section IV and Q_0, the minimal distance obtained is d_{min}=4, so the edge length of the singularity-free cube is a = 8.

By running the optimization algorithm, we find a maximal value d_{min}=5.794 for a center point Q(*38.125, 50, 33*).

We subtract a security value of 0.1 from d_{min}, which becomes d_{min}=5.694.

Figure 8 shows the joint space singularity surface and the maximal joint space singularity-free cube centered at Q(*38.125, 50, 33*) for the manipulator studied.

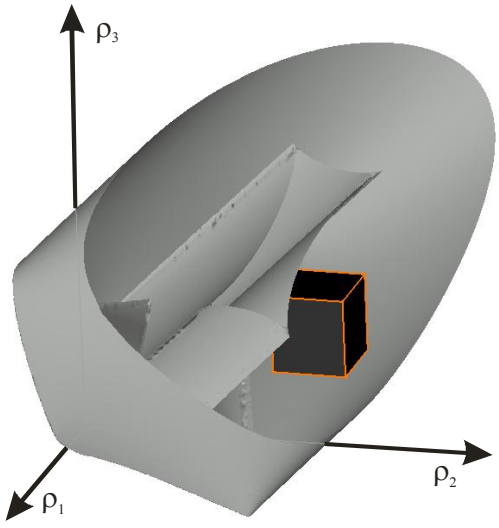

Fig. 8. Joint space singularity curves and maximal joint space singularity-free cube centered at Q(*38.125, 50, 33*).

Figures 9 displays the images by the direct kinematics of the maximal joint space singularity-free cube, which are two separate singularity-free components, one in each aspect of the workspace. The projections of these two components onto the (x,y) plane are plotted in gray in Figure 9. This figure is displayed with the same viewing angle as in Figure 6 to show the difference between the two examples.

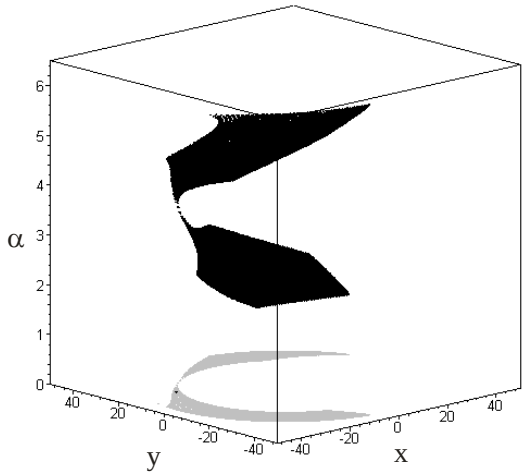

Fig. 9. Images by direct kinematics of the joint space singularity-free cube (in black), and their projection on the (x,y) plane (in gray).

C. Future works

We can see in figures 6 and 9 that the components in the workspace do not have regular forms. Because this study is carried out in the joint space only, it cannot take into account any of the properties, in the workspace, of the image by direct kinematics of the singularity-free cube found.

This work will be extended by taking into account the largest regular volume (cube, cylinder…) inside the workspace components images of the singularity-free cube. The idea will then be to optimize the location of the initial point $Q_0(\rho_{10},\rho_{20},\rho_{30})$ such that the image of the maximal singularity-free cube in the workspace generates a regular volume of maximal size.

VI. Conclusion

A procedure for computing joint space singularities of *3-RPR* parallel manipulators has been presented firstly in this paper. Secondly, a procedure for the determination of maximal joint space singularity-free boxes has been provided.

These two procedures are of interest for planning trajectories in the joint space, and for manipulators design because they provide a tool for choosing the values of the joint limits.

Future work will optimize the choice of the cube center point Q_0 in the joint space in order to maximize the volumes of the workspace components images of the singularity-free cube.

References

[1] M. Arsenault and R. Boudreau, "The synthesis of three-degree-of-freedom planar parallel mechanisms with revolute joints (3-*RRR*) for an optimal singularity free workspace," *Journal of Robotic Systems*, **21** (5), pp.259–274, 2004.

[2] S. Bhattacharya, H. Hatwal, A. Gosh, ''Comparison of an exact and an approximate method of singularity avoidance in platform type parallel manipulators,'' *Mechanism and Machine Theory*, **33** (7), pp. 965–974, 1998.

[3] I. Bonev, D. Zlatanov, and C. Gosselin, "Singularity Analysis of 3-DOF Planar Parallel Mechanisms via Screw Theory," *ASME Journal of Mechanical Design*, vol. 125, no. 3, pp. 573–581, 2003.

[4] D. Chablat and P. Wenger, "Architecture Optimization of a 3-DOF Parallel Mechanism for Machining Applications, the Orthoglide," *IEEE Transactions on Robotics and Automation*, vol. 19(3), pp 403-410, june 2003.

[5] I. Constantinescu, "Détermination de régions exemptes de singularités pour des mécanismes parallèles plans et sphériques à 3 degrés de liberté", Master's Thesis, Department of Mechanical Engineering, Laval University, Québec, Canada,2004**.**

[6] A.K. Dash , I.M. Chen, S.H. Yeo, G. Yang ''Singularity-free path planning of parallel manipulators using clustering algorithm and line geometry,'' *Proc. IEEE International Conference on Robotics & Automation*, Taipei, Taiwan, September 14-19, 2003.

[7] M. Gallant and R. Boudreau,"The Synthesis of Planar Parallel Manipulators with Prismatic Joints for an Optimal, Singularity-Free Workspace", *Journal of Robotic Systems*, Vol. 19, No. 1, pp. 13-24, 2002.

[8] C. Gosselin, and J. Angeles, "Singularity analysis of closed loop kinematic chains," *IEEE Transactions on Robotics and Automation*, vol. 6, no. 3, 1990.

[9] C. Gosselin, J. Sefrioui, and M.J. Richard, "Solution polynomiale au problème de la cinématique directe des manipulateurs parallèles plans à 3 degrés de liberté," *Mechanism and Machine Theory*, vol. 27, no. 2, pp. 107-119, 1992.

[10] R. Hooke, and T.A. Jeeves "Direct search solution of numerical and statistical problems," Journal of the Assoc. Comput. Mach. **8** (2), pp.212-229, 1961.

[11] K. H. Hunt, "Geometry of Mechanisms," *Clarendon Press*, Oxford, 1978.

[12] K.H. Hunt, and E.J.F. Primrose, "Assembly configurations of some In-parallel-actuated manipulators," *Mechanism and Machine Theory*, vol. 28, no. 1, pp.31-42, 1993.

[13] M.L. Husty, M.J.D. Hayes, H. Loibnegger, , "The General Singularity Surface of Planar Three-Legged Platforms", *Advances in Multibody Systems and Mechatronics*, Gerhard-Mercator-Universität, Duisburg, Germany, pp. 203-214, 1999.

[14] C. Innocenti, and V. Parenti-Castelli, "Singularity-free evolution from one configuration to another in serial and fully-parallel manipulators. *Journal of Mechanical design*. 120. 1998.

[15] X. Kong and C.M. Gosselin, "Determination of the uniqueness domains of 3-*RPR* planar parallel manipulators with similar platforms," *Proc. Of the 2000 ASME Design Engineering Technical conferences and Computers and Information in Engineering Conference*, Baltimore, Sept 10-13, 2000.

[16] H. Li and C.M. Gosselin, "Determination of maximal singularity-free zones in the workspace of planar three-degree-of-freedom parallel mechanisms," *Mechanism and Machine Theory*, in press.

[17] H. Li and C.M. Gosselin, "Determination of maximal singularity-free zones in the six-dimensional workspace of the general Gough-Stewart platform," *Mechanism and Machine Theory*, in press.

[18] P.R. Mcaree, and R.W. Daniel, "An explanation of never-special assembly changing motions for 3-3 parallel manipulators," *The International Journal of Robotics Research*, vol. 18, no. 6, pp. 556-574. 1999.

[19] J-P. Merlet, "Trajectory verification in the workspace for parallel manipulators," *International Journal of Robotics Research*, **13** (4), pp. 326–333, 1994.

[20] J-P. Merlet, "Determination of the presence of singularities in 6D workspace of a Gough parallel manipulator," *Proc. ARK, Strobl*, June 29-July 4, pp.39–48, 1998.

[21] J-P. Merlet, *Parallel Robots*, Kluwer Academics, 2000.

[22] J. Sefrioui, and C. Gosselin, "On the quadratic nature of the singularity curves of planar three-degree-of-freedom parallel manipulators," *Mechanism and Machine Theory*, vol. 30, no. 4, pp. 535-551, 1995.

[23] S. Sen, B. Dasgupta, A.K. Mallik, ''Variational approach for singularity-free-path-planning of parallel manipulators,'' *Mechanism and Machine Theory*, **38** (11), pp. 1165–1183, 2003.

[24] P. Wenger, and D. Chablat, "Definition sets for the direct kinematics of parallel manipulators," *Int. Conference on Advanced Robotics*, pp. 859-864, 1997.

[25] P. Wenger, and D. Chablat, "Workspace and assembly modes in fully parallel manipulators: A descriptive study" *Advances on Robot Kinematics*, Kluwer Academic Publishers, pp.117-126, 1998.

[26] M. Zein, P. Wenger, and D. Chablat, "Singular Curves and Cusp Points in The Joint Space of 3-RPR Parallel Manipulators," *Proc. IEEE International Conference on Robotics & Automation*, Orlando, May 2006.